Mirror-Box Pretraining to Evoke Sensorimotor Activation to Facilitate Motor Imagery Detection in Brain-Computer Interface Stroke Rehabilitation

Nina Evetović[1], Roman Rosipal[1], Adrián Hodúr[1], Zuzana Rošťáková[1]

[1]Institute of Measurement Science, Slovak Academy of Sciences

E-mail: nina.evetovic@savba.sk

ABSTRACT: Calibration of motor imagery (MI) brain-computer interface (BCI) systems in stroke patients is challenging due to limited voluntary movement and variable imagery ability. We propose mirror-box (MB) training as a physiologically grounded pretraining strategy to induce contralateral sensorimotor activation and extract subject-specific oscillatory components for MI detection. Electroencephalography (EEG) was recorded during six MB sessions in a chronic post-stroke participant. Parallel Factor Analysis (PARAFAC) was applied to decompose multi-channel EEG into spatial, temporal, and spectral components. Trial-pair normalization relative to the corresponding *rest* segment was used to enhance detection of task-related modulation. Distinct μ and β sensorimotor rhythms were identified, showing significant desynchronization during observation and movement compared to *rest*. An individualized linear discriminant analysis classifier achieved $98.8\% \pm 0.6\%$ accuracy in discriminating *rest* from *motor engagement*. These findings support MB pretraining as a robust strategy for physiologically informed MI-BCI calibration and future BCI Head-Mounted Display rehabilitation applications.

INTRODUCTION

Post-stroke upper limb impairment is a major cause of long-term disability, motivating the development of Brain-Computer Interface (BCI) based neurorehabilitation combined with immersive Head-Mounted Display (HMD) systems [1]. Motor imagery (MI) BCI paradigms rely on the modulation of sensorimotor (SM) rhythms, typically in the alpha and beta frequency bands, and on the reliable detection of these modulations for system control [2, 3].

However, training MI-based BCI-HMD systems in post-stroke patients presents substantial challenges. Calibration based on physical movement of the affected limb is often not feasible. MI can be used as an alternative [1], but its effectiveness strongly depends on the patient's imagery ability, which is highly variable and difficult to verify objectively [4].

To address these limitations, we propose Mirror-Box (MB) training as a physiologically grounded pretraining strategy for identifying oscillatory components suitable for MI-BCI control. MB therapy provides visual feedback of the intact limb to induce the illusion of movement in the paretic limb, reliably activating sensorimotor cortical networks [5]. These responses are stimulus-driven and cannot be voluntarily fabricated [6], making MB training a robust approach for extracting subject-specific sensorimotor generators. Furthermore, MB therapy is an established rehabilitation approach for paretic and hemiparetic patients, leveraging visual feedback to engage sensorimotor networks and facilitate motor recovery [7], making it a valuable addition to BCI-based protocols. While not the primary focus of this work, a study from 2024 demonstrated that MB training can serve as a training tool to improve participants' motor imagery (MI) ability [8], which may be regarded as an additional benefit of the proposed framework.

Electroencephalography (EEG) provides a non-invasive means to capture cortical oscillatory activity associated with motor observation and execution [2, 5]. In this study, we applied tensor decomposition to multi-channel EEG recorded during MB training to extract individualized oscillatory components corresponding to sensorimotor activity. Using Parallel Factor Analysis (PARAFAC), we preserved the multidimensional structure of the data across space, time, and frequency, enabling identification of μ and β rhythms modulated during MB training [5, 9].

The aim of this paper is threefold: (i) to extract physiologically interpretable oscillatory components reflecting sensorimotor generators elicited by MB training, (ii) to quantify their discriminative capacity by constructing a linear discriminant analysis (LDA) classifier to differentiate rest from motor-related states, and (iii) to propose MB training as a structured strategy for training and calibrating MI-based BCI models. By using MB training to elicit robust and verifiable sensorimotor activation, we aim to establish a principled framework for feature extraction that can support future BCI-HMD motor neurorehabilitation applications and contribute to a deeper understanding of the neural mechanisms underlying MB therapy.

MATERIALS AND METHODS

Experimental Paradigm and Protocol:

We recorded six MB training sessions. Each experimental session began with baseline resting state recordings consisting of 2 minutes with eyes closed (EC) followed by 2 minutes with eyes open (EO). During the EO condi-

tion, the participant was instructed to fixate on a centrally positioned plus sign (+) to minimize ocular artifacts.

The main part of each session consisted of two MB training blocks. In the first block, referred to as *Visual Left Hand* (VLH), the participant performed movements with the unaffected upper limb while the paretic limb was positioned behind the mirror. The participant observed the reflection of the healthy hand in the mirror, creating the visual illusion of movement in the affected limb. In the second block, *Visual Both Hands* (VBH), the participant again observed the reflection of the healthy hand but simultaneously attempted to move the affected limb in synchrony with the observed movement.

Each block began with a 30 s eyes open resting period. A technician seated opposite the participant demonstrated three to four repetitions of each movement, after which the participant performed the same movement at a self-paced rhythm for approximately 7 to 10 repetitions. Consecutive movement types were separated by a 15 s eyes open resting interval. This procedure was repeated until all 10 movement types, each comprising rest, observation, and movement periods, were completed. Each block concluded with a final 30 s eyes open resting period. After completion of both training blocks, additional 2 minute resting state recordings were obtained under EO and EC conditions.

Each trial was evaluated for separability between *rest* and motor-related conditions (*observe* and *move*), based on mirror neuron mechanisms that support activation during both action observation and execution. These phases were present in both VLH and VBH blocks, but were later unified into functional labels (*rest*, *observe*, *move*) rather than block-specific terminology. Both VLH and VBH were included to increase variability by capturing unilateral and bilateral motor activations, improving generalizability of the learned representations; therefore, all blocks were jointly used for classifier training.

Each mirror box training block included 10 distinct upper limb movements, with following instructions:

- **Elbow-Supported Hand Lift** – Elbow resting on the table; lift the hand while keeping the forearm in contact.
- **Palm Rotation** – Forearm on the table; rotate the palm upward and downward.
- **Palm Lift** – Rest of the hand on the table; lift the palm upward.
- **Finger Spread and Close** – Spread the fingers apart and then bring them together.
- **Fist Closure** – Palm up on the table; close fingers into a fist with the thumb inside.
- **Ball Roll** – Roll a ball on the table using the palm; lift fingers as the ball reaches the bottom of the palm.
- **Bottle Grasp and Release** – Grasp a bottle, release it, then return the hand to the table.
- **Finger Pinch** – Palm up on the table; pinch the fingers together.
- **Thumb-to-Finger Taps** – Palm up; sequentially touch each finger with the thumb from index to little finger and back.
- **Cube Manipulation** – Palm down; move a cube once using only the thumb and index finger, then move it back using all five fingers.

Participant Characteristics and Dataset Description:

The study included a single participant, a 70-year-old individual with a 10-year history of spastic hemiparesis affecting the right upper limb more prominently. The participant was able to walk independently and demonstrated normal speech and cognitive function. They were capable of following instructions and managing the training session schedule without difficulty.

EEG signals were recorded continuously throughout each session, including baseline resting-state periods with EC and EO, as well as during two MB training blocks. The dataset therefore includes both resting-state and task-related EEG segments, providing sufficient temporal coverage for the analysis of SM rhythms.

EEG Acquisition and Recording Setup:

Continuous EEG activity was recorded using the wireless g.Nautilus PRO FLEXIBLE system, an FDA-cleared device. The system was equipped with 19 Ag/AgCl active wet electrodes arranged according to the international 10–20 system and integrated into an 19-channel g.tec cap and amplifier. The EEG cap was positioned following the manufacturer's instructions. Signals were sampled at 250 Hz.

A1 served as the reference electrode and AFz as the ground. For subsequent signal processing, recordings were re-referenced to the the A2 electrode, resulting in the referencing with the average of both earlobe electrodes, A1 and A2, using the formula $(\mathrm{A1}+\mathrm{A2})/2$.

Signal Preprocessing Pipeline:

The EEG recordings were initially converted to EDF format and preprocessed using Brain Vision Analyzer 2.3.03 [10]. The preprocessing steps included:

(a) identification and interpolation of channels with missing or corrupted data;

(b) a semi-automatic threshold-based procedure to detect general artifacts, followed by visual inspection to ensure accurate marking; and

(c) detection of electromyographic (EMG) artifacts prior to data export.

Subsequently, the data were processed in MATLAB [11], where the continuous EEG signals were segmented into 2 s epochs with a 500 ms moving window. From these epochs, features including fractal, harmonic, and raw spectral components were extracted using an Irregular-Resampling Auto-Spectral Analysis (IRASA) approach [12] with a Hann window.

Parallel Factor Analysis:

Parallel Factor Analysis (PARAFAC) is a tensor decomposition method that extends matrix factorization techniques to multi-way data structures [9]. In contrast to matrix-based approaches that require unfolding higher-order data into two-dimensional representations, PARAFAC preserves the intrinsic multi-dimensional structure of the data, which is particularly advantageous

for EEG signals that naturally exhibit spatial, temporal, and spectral modes [13, 14].

Let $\mathbf{X} \in \mathbb{R}^{I \times J \times K}$ denote a three-way tensor constructed from EEG power spectral density estimates across I time segments, J electrodes, and K frequency bins. The PARAFAC model decomposes $\mathbf{X}$ into a sum of F rank-one tensors:

$$\mathbf{X} \approx \sum_{f=1}^{F} \mathbf{a}_f \circ \mathbf{b}_f \circ \mathbf{c}_f + \mathbf{E}, \tag{1}$$

where $\mathbf{a}_f$, $\mathbf{b}_f$, and $\mathbf{c}_f$ represent the temporal, spatial, and spectral loading vectors of the f-th component, respectively, $\circ$ denotes the vector outer product, and $\mathbf{E}$ is the residual error tensor [9]. Each component therefore corresponds to a tri-linear pattern, often referred to as an "atom," that jointly characterizes space–time–frequency signatures in the EEG data [14].

Additional constraints may be incorporated to reflect prior knowledge about EEG structure. In particular, non-negativity constraints in selected modes can enhance interpretability when working with amplitude spectral representations [15].

In line with previous applications of PARAFAC to MB therapy and SM rhythm analysis [5], the extracted loading matrices were interpreted as temporal activations, spatial topographies, and spectral profiles of oscillatory EEG components. This space–time–frequency decomposition enables tracking of task-related modulations and longitudinal changes in SM oscillatory activity.

PARAFAC for Sensorimotor Rhythm Identification:

The preprocessed EEG data were arranged into a three-way tensor with dimensions corresponding to channels (spatial), time, and frequency. PARAFAC decomposition was applied to extract task-related oscillatory components across these modes [9, 14].

The resulting loading matrices represented temporal activations, spatial topographies, and spectral profiles of each component (as shown in Fig. 1). Components exhibiting spectral peaks in the alpha (7–12 Hz) and beta (13–30 Hz) bands over sensorimotor regions were identified as SM rhythms and analyzed for task-related modulation during MB training [5].

Each component was visually inspected, and only those localized to the sensorimotor area, within the expected frequency ranges, and consistent with the oscillatory patterns observed in the data were selected. Components not meeting these criteria were discarded.

Individualized Modeling Using Oscillatory SM Components:

After selecting the SM components relevant to motor activity during the task, a linear discriminant analysis (LDA) classifier was constructed. LDA has been widely used in EEG and motor imagery classification due to its simplicity, efficiency, and robust performance in discriminating sensorimotor states from oscillatory EEG features [16]. An individualized LDA classifier was trained to discriminate between *rest* and *active motor engagement*, where the active class combined both observation and movement segments.

The model was trained using data from 12 separate blocks, corresponding to one cycle of 10 exercises, each comprising rest, observation, and movement segments. To ensure robust performance estimation, a leave-one-out cross-validation approach was applied. In each fold, 11 blocks were used for training and the remaining block was used for testing.

To account for baseline variability and the task structure, trial-by-trial normalization was applied. Specifically, each trial was normalized using the resting-state data from the same trial, providing a precise baseline for detecting changes in sensorimotor activity during observation and movement. This procedure ensured that task-related neural dynamics could be reliably captured across trials.

Statistical Analysis:

For each extracted sensorimotor component, scores were computed by projecting the EEG data onto the atom's spatial and frequency weights, providing a measure of how strongly the component was expressed in each trial. These scores were then averaged across trials within each block to obtain condition-specific values for *rest*, *observe*, and *move* (12 blocks across six sessions).

Statistical comparisons between *rest*vs *move* and *rest* vs *observe* were conducted using the Wilcoxon signed-rank test, with Bonferroni correction applied to account for multiple comparisons. Significance was reported at corrected confidence levels of $p < 0.05$, $p < 0.01$, and $p < 0.001$. A direct comparison between *observe* and *move* was not performed, as both were grouped as motor-related conditions and evaluated only relative to the *rest* baseline, which is the primary reference in sensorimotor rhythm analysis and the proposed framework.

RESULTS

Detection of Oscillatory SM Rhythms:

Figure 1 presents the participant's SM oscillatory rhythms extracted using PARAFAC decomposition. Five distinct components were identified, all localized over the sensorimotor cortex. Prior to visualization, spatial weight vectors were zero padded to increase the density of displayed samples and avoid visual broadening due to interpolation. The padding was removed after rendering and did not influence the computed component structure. Two components representing the μ rythm were separated despite sharing the same spectral peak at 11.8 Hz, indicating spatially distinct sources.

In addition to the μ components, three distinct beta-range components were identified at 13.7 Hz, 16.7 Hz, and 19.5 Hz. The 13.7 Hz component corresponds to SMR, whereas the components at 16.7 Hz and 19.5 Hz represent higher β sub-bands within the sensorimotor rhythm.

Sensorimotor Atom Scores:

In Figure 2, we show the computed atom scores across the *rest*, *observe*, and *move* conditions. For each fre-

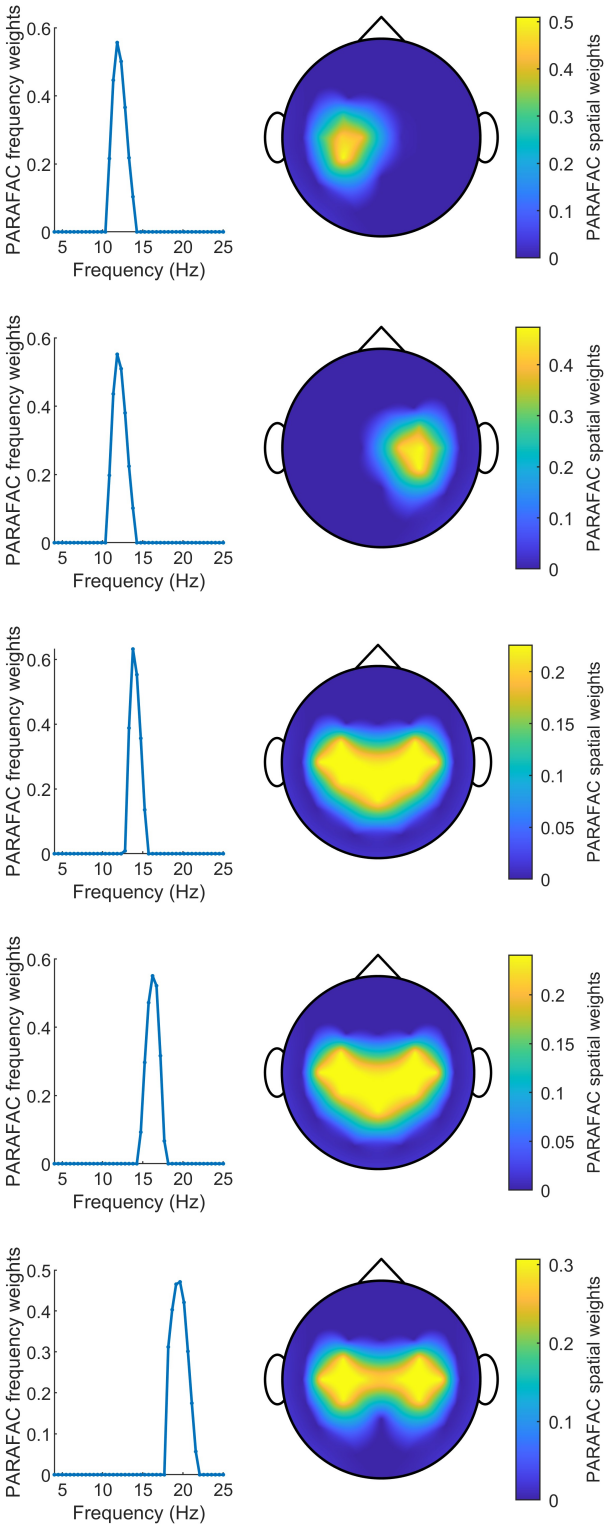

Figure 1: Five SM oscillatory components identified using PARAFAC decomposition. Each component is represented by its frequency weights (left) and the corresponding scalp topography of spatial weights (right). The components correspond, respectively, to the left μ rhythm (11.8 Hz), right μ rhythm (11.8 Hz), SMR (13.7 Hz), β 1 (16.7 Hz), and β 2 (19.5 Hz).

quency band, mean t-scores were calculated for all extracted atoms and averaged across blocks. Boxplots illustrate the distributions of these scores across conditions.

The scores were lower during *move* and *observe* compared to *rest*, indicating that the extracted atoms captured task-related sensorimotor activity and possibly reflected event-related desynchronization (ERD). Wilcoxon signed-rank tests (Bonferroni-corrected) confirmed that these differences were significant for most frequency bands, supporting the reliability of the atoms in reflecting condition-specific modulation of sensorimotor networks.

The most statistically significant ERD across trials was observed in the μ rhythm. An example of this desynchrony for a representative movement averaged over all trials is shown in Fig. 3.

LDA Classification of Sensorimotor States:

The individualized LDA classifier demonstrated excellent performance in discriminating *rest* versus *motor engagement*. Across cross-validation folds, the classification accuracy was $98.8\% \pm 0.6\%$, indicating highly consistent predictions. The mean area under the ROC curve (AUC) was 0.990 ± 0.0, reflecting near-perfect discrimination between classes. The effect size, quantified using Cohen's d, was $\mathrm{d} = 2.374 \pm 0.0$, indicating a large separation between rest and motor-related states.

DISCUSSION

In this study, we investigated the use of MB pretraining to identify SM oscillatory components relevant for MI detection in a BCI-HMD paradigm. Our results build on previous work comparing MB-induced EEG activity with signals recorded during robotic splint-assisted movements, we observed overlapping SM generators, supporting the physiological validity of mirror-based activation and demonstrating substantial similarity between atoms extracted from MB training and those elicited by robotic arm movements [5, 17].

Unlike these earlier, more heuristic approaches, the present study applied a LDA classifier to evaluate whether the identified SM components could reliably discriminate motor-related states in new participants. This methodological refinement allowed us not only to confirm the presence of MB-related oscillatory generators but also to quantify their discriminative capacity, providing evidence that these components capture physiologically meaningful SM activity.

Inspection of the extracted components revealed distinct left and right μ rhythms. The right μ component likely reflects contralateral SM activation associated with hand movement. In contrast, the left μ component may represent cortical processes related to MB training, specifically the visual observation of the hand in the mirror, potentially engaging mirror neuron system mechanisms through visually induced motor simulation.

It has been proposed that multiple β rhythms contribute to motor processing and may serve functionally distinct roles. Specifically, different β sub-bands have been

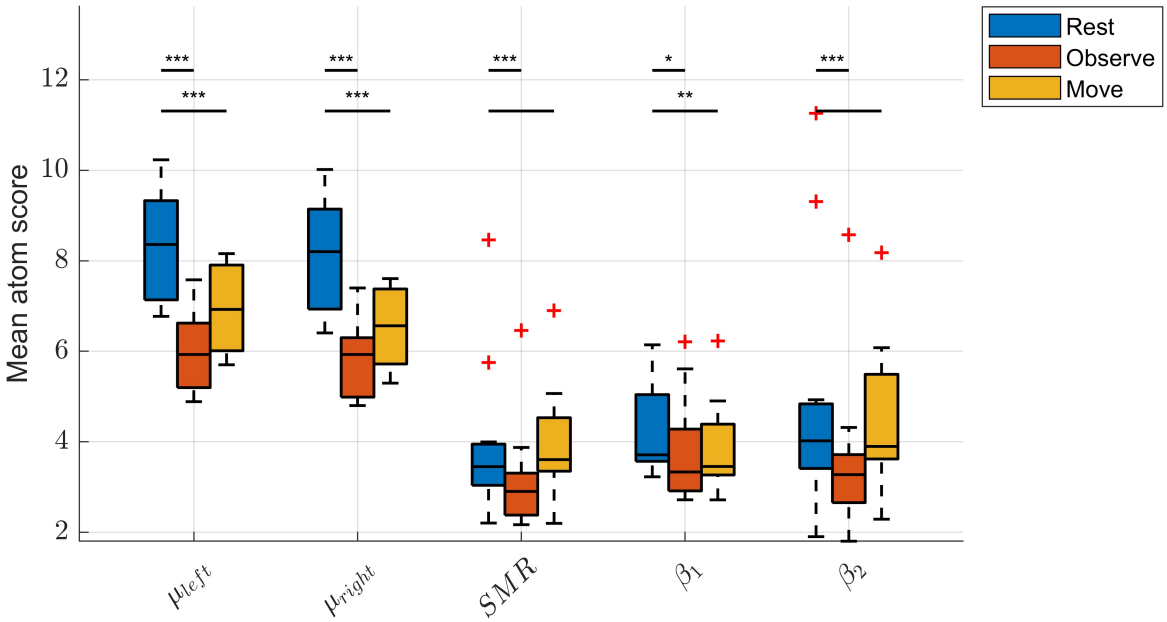

Figure 2: Five SM atom scores for *rest*, *observe* and *move* conditions averaged per block. Asterisks indicate statistically significant differences after correction for multiple comparisons: * $p < 0.05$, ** $p < 0.01$, and *** $p < 0.001$.

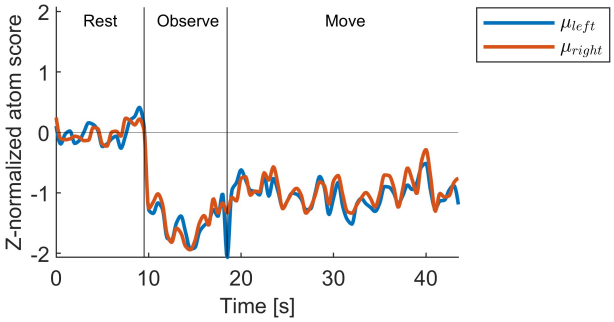

Figure 3: Z-normalized scores of the left and right μ components across *rest*, *observe*, and *move* segments. Scores were normalized relative to the corresponding *rest* baseline. The figure illustrates desynchronization for one representative movement, averaged across all sessions for the same movement task.

reported to exhibit divergent modulation patterns during motor tasks, with some showing ERD while others demonstrate synchronization. These sub-bands may also differ in their peak frequency and spatial distribution, suggesting distinct underlying neural generators and functional relevance.

In our study, the μ rhythm exhibited clear desynchronization during both observation and movement conditions, consistent with engagement of the SM cortex. In contrast, β band activity showed stronger desynchronization during observation than during movement. This difference likely arises from the design of the movement blocks: each movement consisted of approximately ten repetitions, and β rhythms are known to resynchronize after movement, which reduces observable desynchronization in averaged epochs. In comparison, μ rhythms fluctuate but remain desynchronized over longer periods, allowing more reliable detection of task-related modulation.

Statistical analysis supported these findings, with significant desynchronization observed in both observation and movement conditions relative to rest for the μ rhythms, whereas β band effects were less consistent.

These findings highlight the importance of an appropriate baseline and task protocol to accurately capture oscillatory dynamics. Moreover, our results demonstrate that careful identification of subject-specific SM atoms, combined with individualized classifier training, can yield high-performance detection of *motor engagement*, as reflected in the near-perfect LDA accuracy.

Overall, these results support the use of MB pretraining as a robust strategy for extracting physiologically meaningful EEG features in patients with limited motor function. By providing stimulus-driven activation that does not rely on voluntary movement, MB training enables the identification of SM generators that can subsequently be used to train MI-based BCI models, facilitating reliable detection of motor imagery in rehabilitation contexts. Future work will extend these findings to online BCI-HMD paradigms and investigate their applicability across a larger cohort of post-stroke patients.

CONCLUSION

This study demonstrates that MB pretraining combined with PARAFAC decomposition enables extraction of physiologically meaningful, subject-specific SM (μ and β) components in a chronic post-stroke participant. The identified atoms showed significant task-related desynchronization and enabled near-perfect discrimination between rest and *motor engagement* using an individualized LDA classifier (98.8% accuracy, AUC $= 0.990$).

These findings support MB training as a robust, stimulus-driven strategy for calibrating MI-based BCI models when voluntary movement is limited.

The use of multiple distinct movements was intended to capture a broader range of motor-related neural activations and improve the generalizability of the learned representations. In the current work, these movements were combined into a binary classification framework (*motor engagement* vs. *rest*), consistent with the intended application of pretraining spatial filters. However, extending this approach to multi-class classification between different movements represents a valueble direction for future work and could provide further insight into the separability and specificity of the extracted motor patterns. A direct comparison between VLH and VBH conditions was not performed in the present study, as the primary objective was to distinguish *motor engagement* from *rest* for pretraining purposes. However, comparative analysis between unilateral and bilateral conditions may provide additional insight into lateralized versus distributed sensorimotor activation and will be considered in future work.
A key limitation of the present study is the absence of validation in an MI-based setting, which restricts the ability to directly assess the effectiveness of the proposed pretraining strategy in the intended application domain. Additionally, the experimental design limits the investigation of β synchrony and the precise temporal interplay of SM rhythms, particularly due to the repeated movement structure and epoch-based averaging.
Therefore, future work will evaluate the consistency of the identified SM generators in BCI-HMD settings, assess performance without trial-wise normalization, and further examine the temporal dynamics and functional roles of distinct μ and β sub-bands across repeated movements. Overall, this study represents a preliminary step toward improving MI-based BCI performance, with validation in MI contexts identified as a critical next step.

FUNDING

This research was supported by the EU NextGenerationEU initiative through the Recovery and Resilience Plan for Slovakia under project No. 09I03-03-V04-00205 (Z.R.) and project No. 09I03-03-V04-00443 (R.R. and A.H.). Additional funding was provided by the European Commission through the HORIZON-MSCA 2022-DN, 101118964-DONUT project. This work was also supported by the Slovak Research and Development Agency under grant APVV-21-0105 (TInVR) and VEGA 2/0094/26.

REFERENCES

[1] Khan MA, Das R, Iversen HK, Puthusserypady S. Review on motor imagery based BCI systems for upper limb post-stroke neurorehabilitation: From designing to application. Computers in Biology and Medicine. 2020;123.
[2] Pfurtscheller G, Neuper C. Motor imagery activates primary sensorimotor area in humans. Neuroscience Letters. 1997;239(2-3):65–68.
[3] McFarland D, Wolpaw J. EEG-based brain–computer interfaces. Current Opinion in Biomedical Engineering. 2017;4:194–200.
[4] Chen YY, Lambert KJ, Madan CR, Singhal A. Mu oscillations and motor imagery performance: A reflection of intra-individual success, not inter-individual ability. Human Movement Science. 2021;78:102819.
[5] Rosipal R, Porubcová N, Barančok P, Cimrová B, Farkaš I, Trejo LJ. Effects of mirror-box therapy on modulation of sensorimotor EEG oscillatory rhythms: A single-case longitudinal study. Journal of Neurophysiology. 2019;121(2):620–633.
[6] Oberman LM, McCleery JP, Ramachandran VS, Pineda JA. EEG evidence for mirror neuron activity during the observation of human and robot actions: Toward an analysis of the human qualities of interactive robots. Neurocomputing. 2007;70(13-15):2194–2203.
[7] Gandhi DB, Sterba A, Khatter H, Pandian JD. Mirror Therapy in Stroke Rehabilitation: Current Perspectives. Therapeutics and Clinical Risk Management. 2020;Volume 16:75–85.
[8] Gómez DMC, Braidot AAA. Improving motor imagery through a mirror box for BCI users. Journal of Neurophysiology. 2024;131(5):832–841.
[9] Bro R. Parafac: Tutorial and applications. Chemometrics and Intelligent Laboratory Systems. 1997;38(2):149–171.
[10] Brain Products GmbH. *Brainvision analyzer*. Version 2.3.0. Computer software. Gilching, Germany, 2023.
[11] The MathWorks Inc. *Matlab version 24.1 (r2024a)*. Natick, Massachusetts, United States: The MathWorks Inc., 2024.
[12] Wen H, Liu Z. Separating fractal and oscillatory components in the power spectrum of neurophysiological signal. Brain Topography. 2016;29(1):13–26.
[13] Cong F, Lin QH, Kuang LD, Gong XF, Astikainen P, Ristaniemi T. Tensor decomposition of EEG signals: A brief review. Journal of Neuroscience Methods. 2015;248:59–69.
[14] Miwakeichi F, Martínez-Montes E, Valdés-Sosa PA, Nishiyama N, Mizuhara H, Yamaguchi Y. Decomposing EEG data into space-time-frequency components using parallel factor analysis. NeuroImage. 2004;22(3):1035–1045.
[15] Rošťáková Z, Rosipal R. Determination of the number of components in the PARAFAC model with a nonnegative tensor structure: A simulated EEG data study. Neural Computing and Applications. 2022;34(17):14793–14805.
[16] Lotte F et al. A review of classification algorithms for EEG-based brain–computer interfaces: A 10 year update. Journal of Neural Engineering. 2018;15(3):031005.
[17] Rosipal R, Porubcová N, Cimrová B, Farkaš I. Mirror-therapy as a way to start bci robot-assisted rehabilitation: A single case longitudinal study of a patient with hemiparesis. In: 7th International BCI Meeting: BCIs: Not Getting Lost in Translation, Asilomar Conference Center, Pacific Grove, California, USA. 2018, 113.